

Supplementary Material for

3D Porous Catalysts for Plasma-Catalytic Dry Reforming of Methane: How Does the Pore Size Affect the Plasma-Catalytic Performance?

Jinxin Wang^{a,b}, Kaimin Zhang^b, Annemie Bogaerts^{a*} and Vera Meynen^{b,c*}

^aPlasma Lab for Applications in Sustainability and Medicine - ANTwerp, Department of Chemistry, University of Antwerp, Universiteitsplein 1, 2610 Wilrijk, Antwerp, Belgium

^bLaboratory of Adsorption and Catalysis, Department of Chemistry, University of Antwerp, Universiteitsplein 1, 2610 Wilrijk, Antwerp, Belgium

^cFlemish Institute for technological research, VITO NV, Boeretang 200, 2400 Mol, Belgium

*Email: annemie.bogaerts@uantwerpen.be; vera.meynen@uantwerpen.be

Results

Table S1. Composition details of the CuO catalysts.

| Samples | Al (wt%) | Si (wt%) | Ca (wt%) | Cu (wt%) |
|----------|----------|----------|----------|----------|
| CuO-10 | | 0.41 | 0.24 | 99.35 |
| CuO-50 | 0.42 | 0.34 | 0.21 | 99.03 |
| CuO-100 | 0.35 | 0.26 | | 99.39 |
| CuO-600 | 0.34 | 0.43 | | 99.22 |
| CuO-1000 | | 0.31 | | 99.69 |
| CuO-2000 | 0.23 | 0.29 | 0.74 | 98.75 |

Chemicals with Al or Ca were not used in the synthesis. The presence of Al and Ca could be attributed to the contamination during the EDX measurement process.

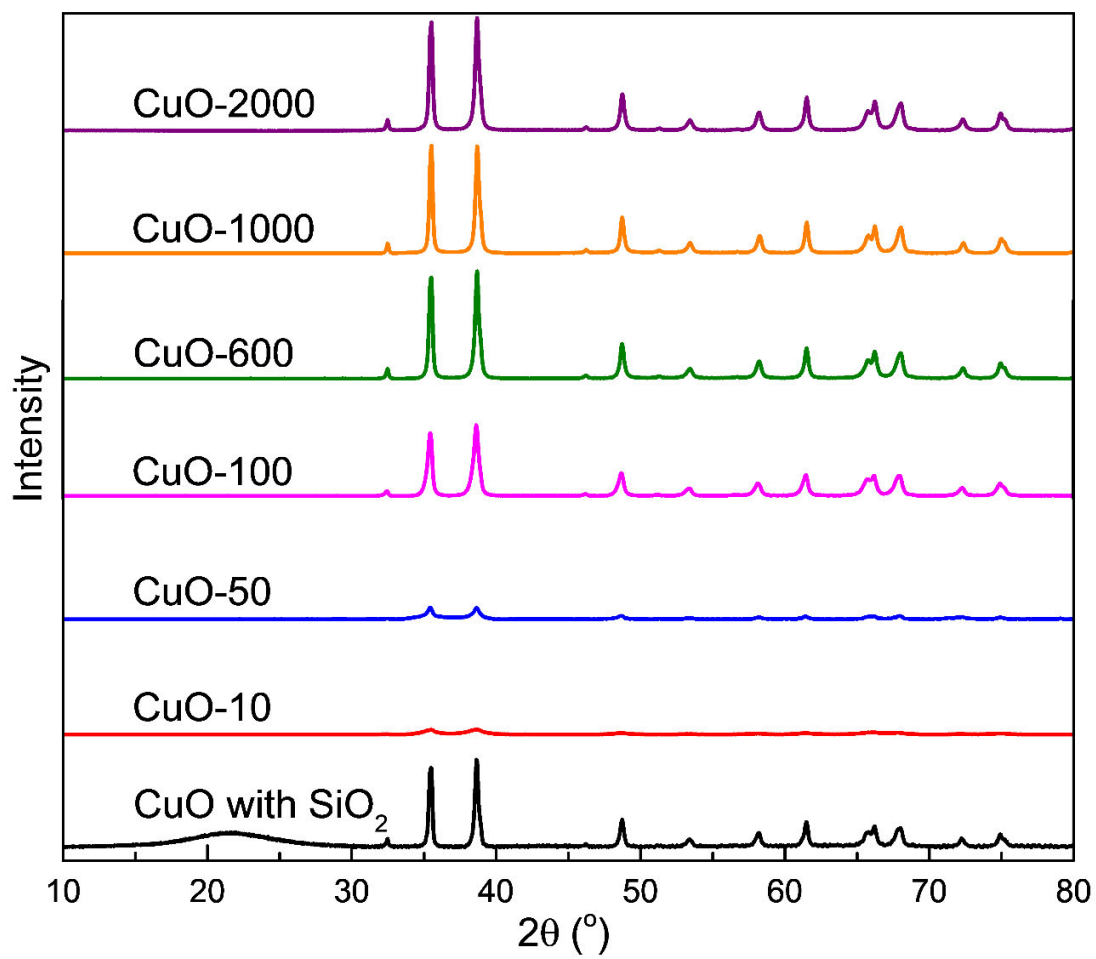


Figure S1. XRD patterns of the 3D porous CuO samples.

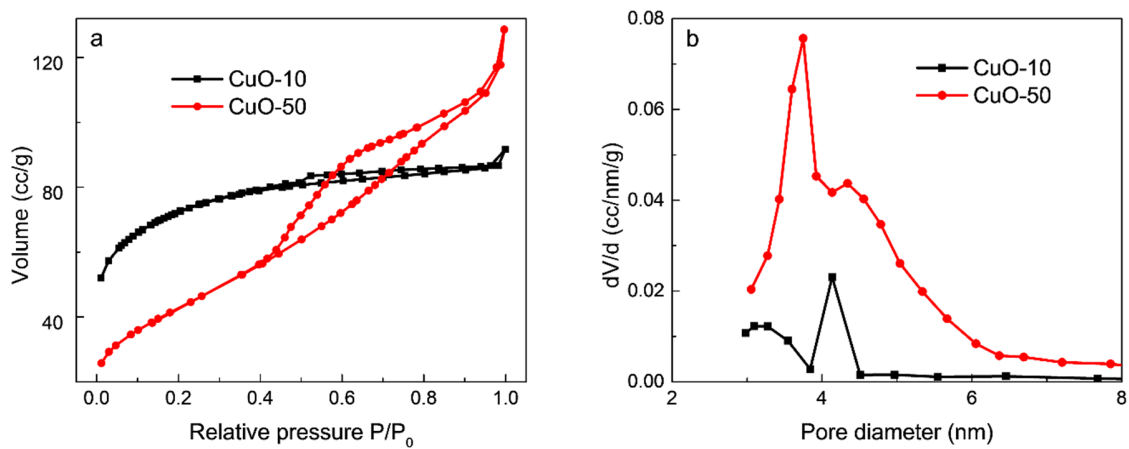


Figure S2. (a) Isotherms of CuO-10 and CuO-50. (b) Pore size distribution of 3D porous CuO samples obtained by N_2 -sorption (BJH desorption branch).

In the Figure S2, it should be noted that the sharp pore size distribution peaks at 3.7 nm of CuO-50 and at 4.1 nm of CuO-10 in Figure S2 (b) should be phantom peaks due to the lower closure point of nitrogen isotherms at 0.42 P/P_0 . It can be deduced from the isotherms that the pore neck size of CuO-10 is too small (< 2 nm) to calculate the right distribution by BJH desorption branch.

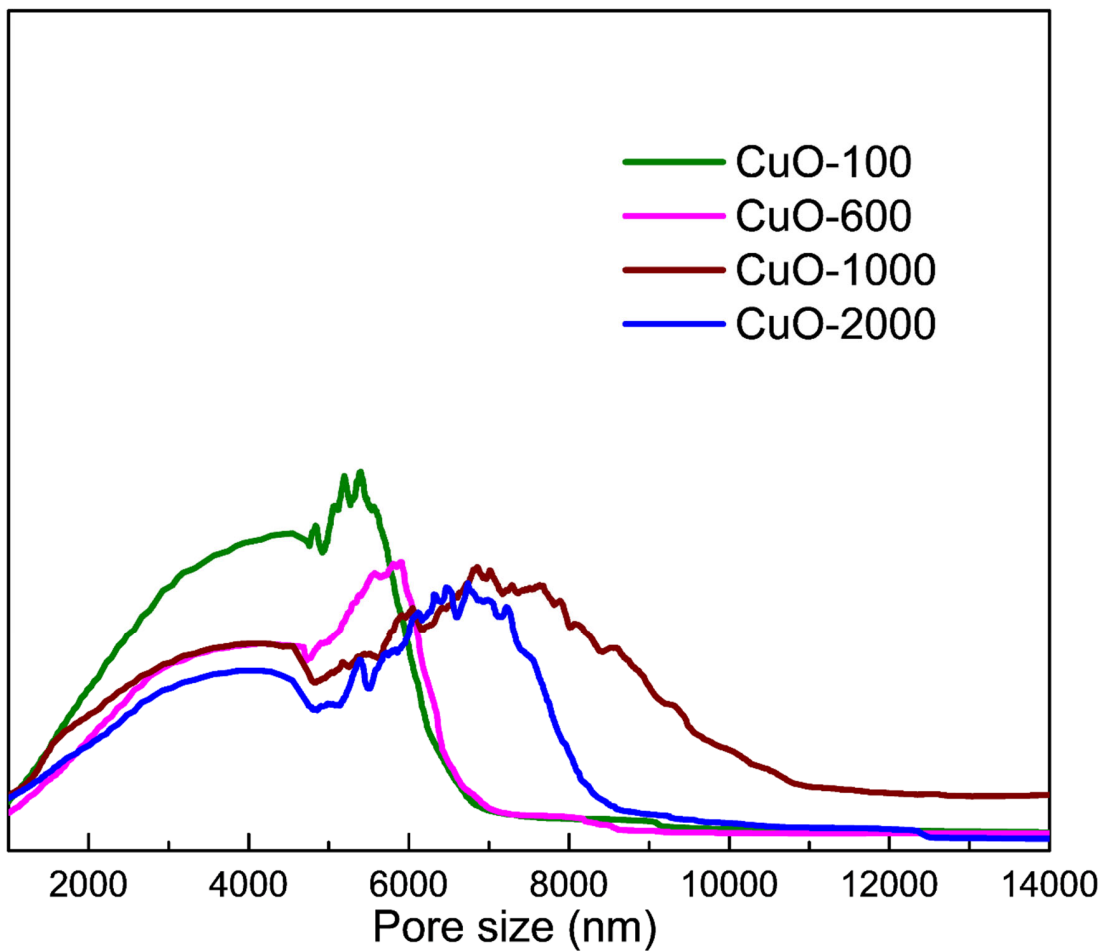


Figure S3. Pore size distribution of 3D porous CuO-100, CuO-600, CuO-1000 and CuO-2000 obtained by mercury intrusion at the micrometer scale.

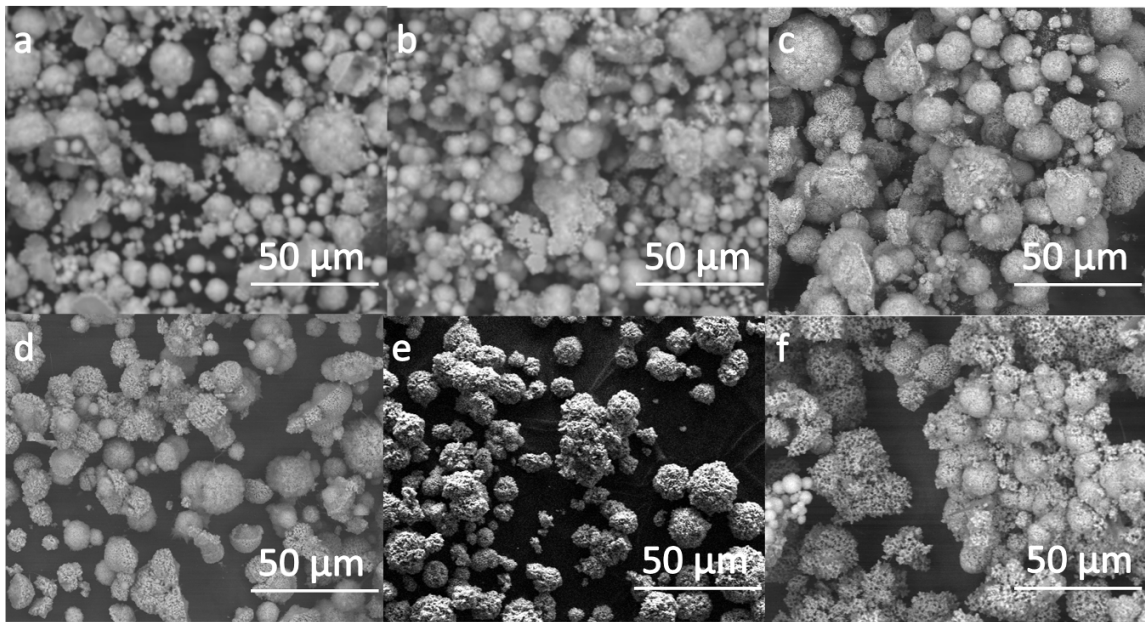


Figure S4. SEM of 3D porous particles (a) CuO-10, (b) CuO-50, (c) CuO-100, (d) CuO-600, (e) CuO-1000, (f) CuO-2000.

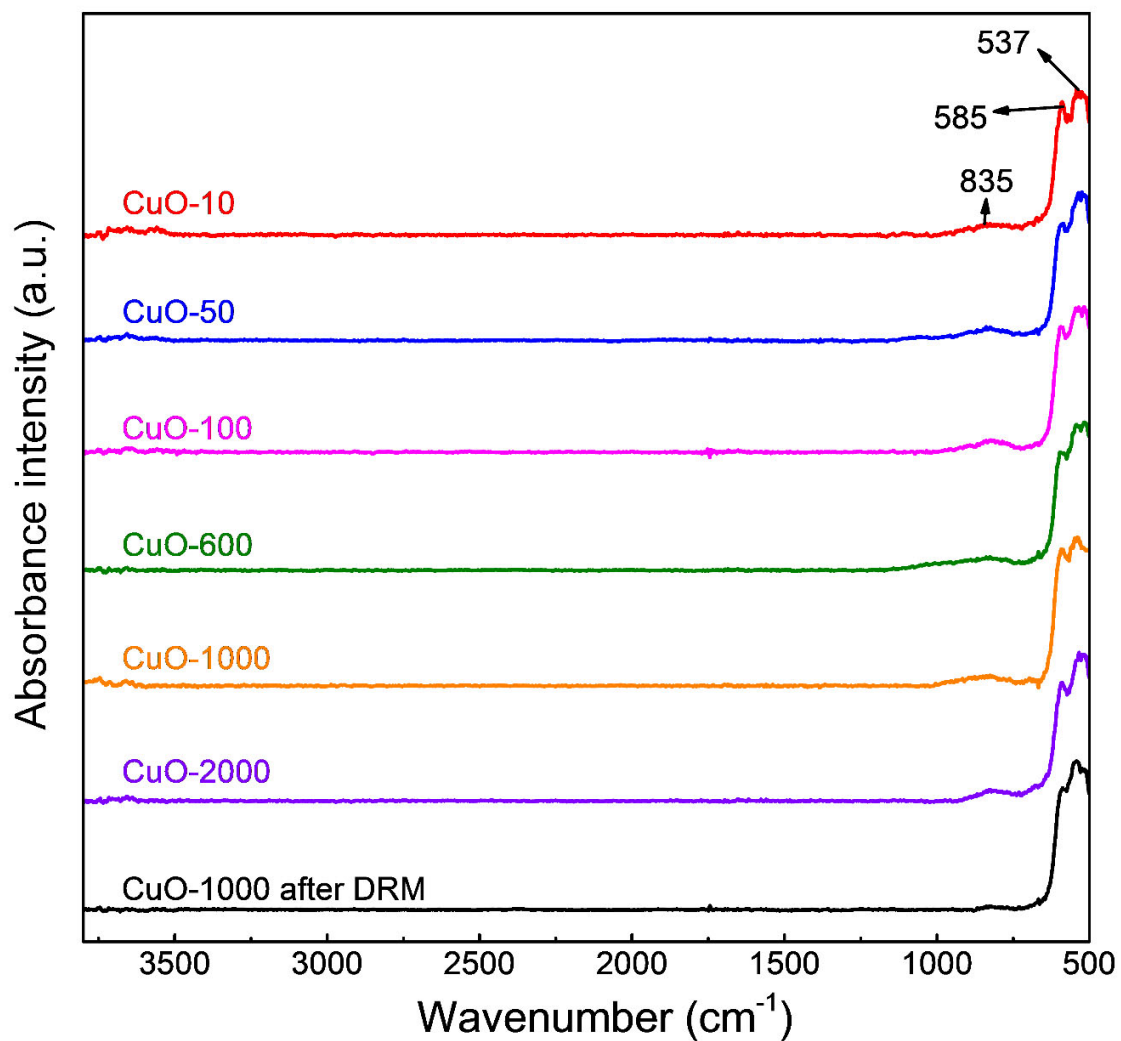


Figure S5. Infrared (DRIFT) spectra of 3D porous CuO, recorded as a 0,5wt% dilution in KBr and after flowing argon at 80 ml/min for 30 minutes at room temperature.

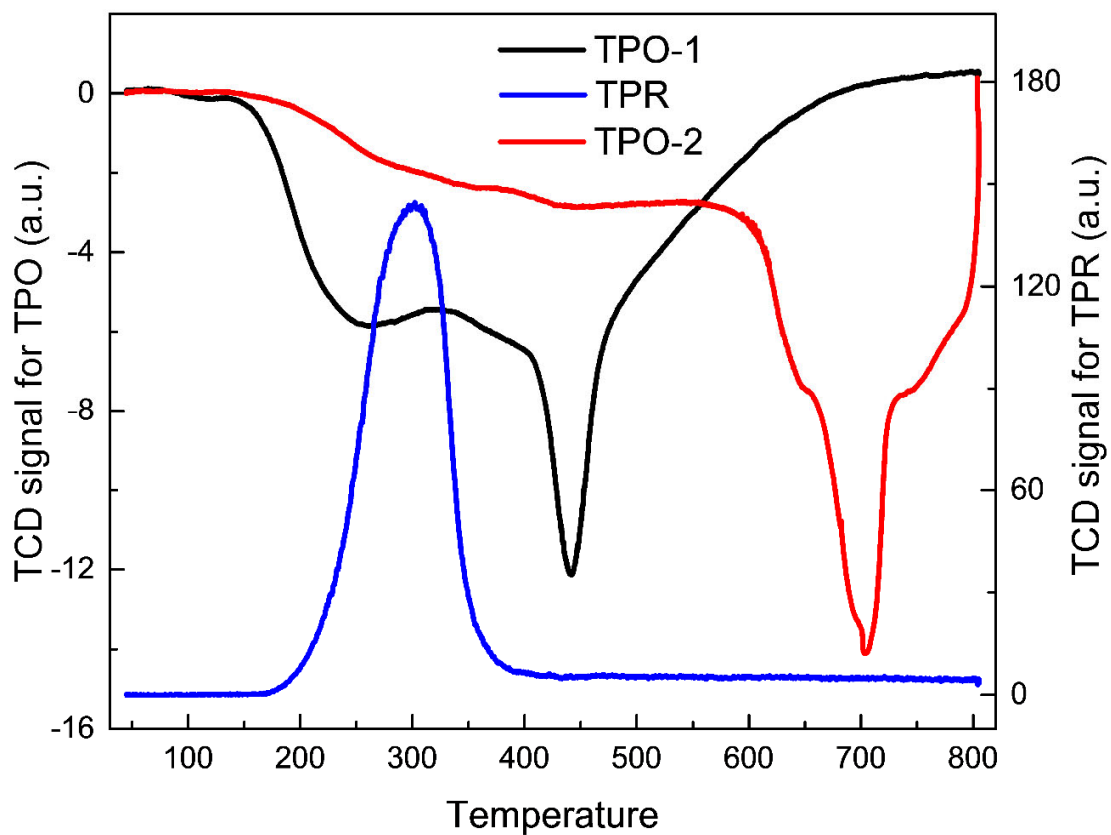


Figure S6. Results of TPO-TPR-TPO of 3D porous samples after reduction in tube furnace at 450 °C.

The CuO samples were calcined at 600 °C and reduced at 450 °C during the syntheses and reduction. The 800 °C high temperature treatments of TPO-1 and TPR changed the oxidation temperature in TPO-2.

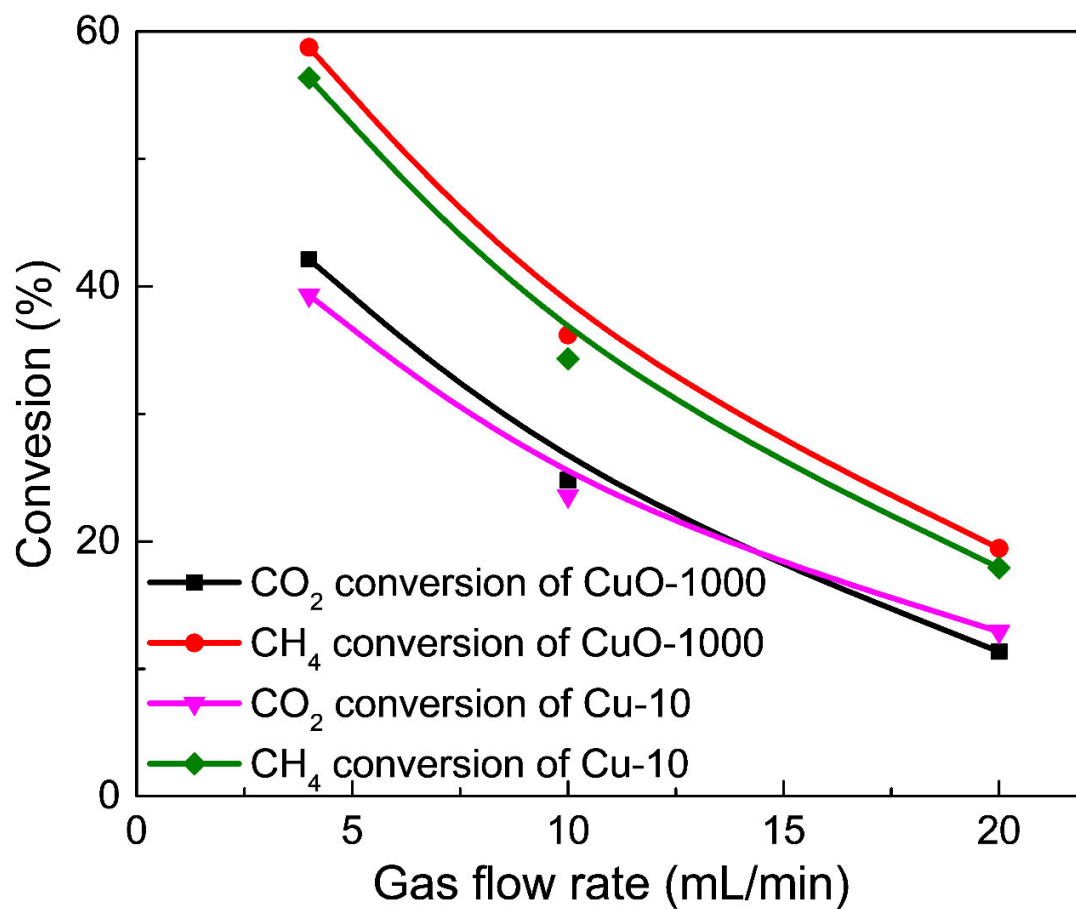


Figure S7. Conversion of CH₄ and CO₂ in plasma-catalytic dry reforming with two representative samples, i.e., Cu-10 and CuO-1000, at feed gas flow rates of 4 mL/min, 10 mL/min and 20 mL/min.

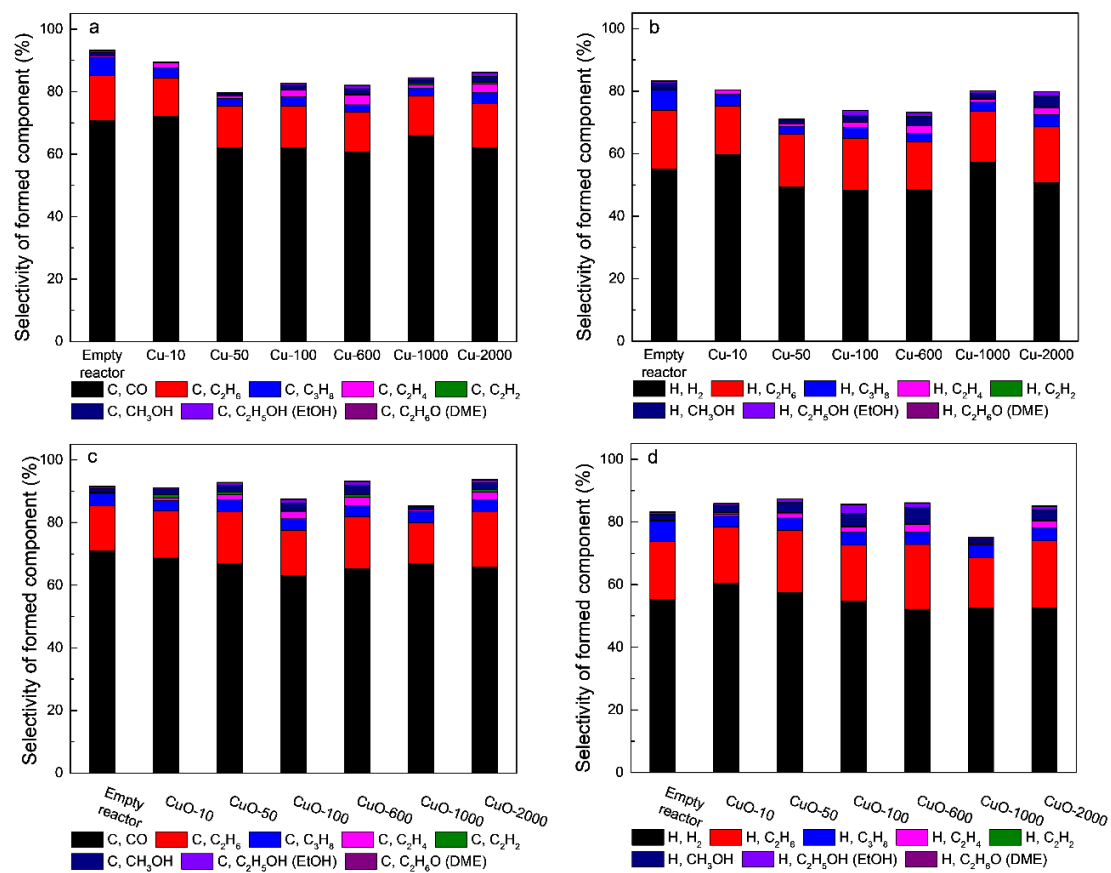


Figure S8. Product carbon-based selectivities and carbon mass balance in plasma-catalytic dry reforming with different pore sizes of 3D porous Cu (a) and CuO (c) samples, and hydrogen-based selectivities and hydrogen mass balance in plasma-catalytic dry reforming with different pore sizes of 3D porous Cu (b) and CuO (d) samples.

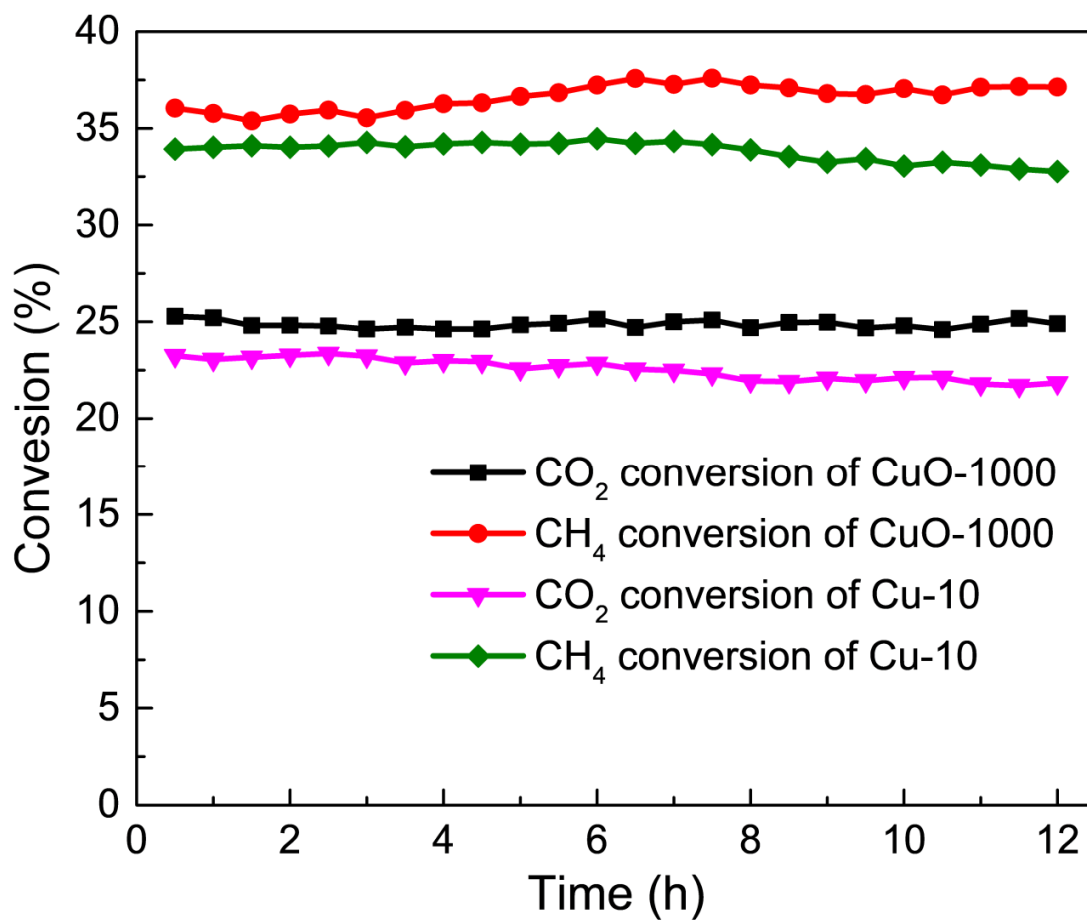


Figure S9. Conversion of CH₄ and CO₂ in plasma-catalytic dry reforming for 12 h with Cu-10 and CuO-1000.

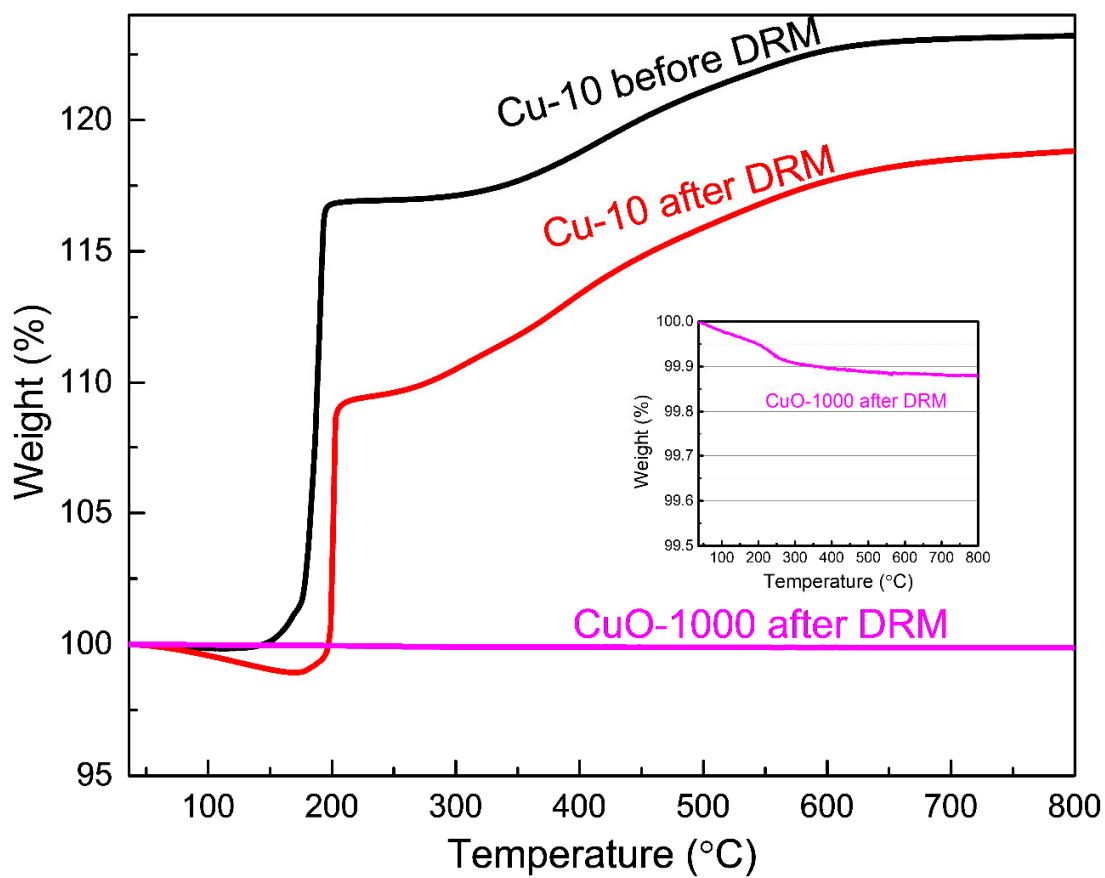


Figure S10. TGA in O₂ of Cu-10 before DRM, Cu-10 after DRM and CuO-1000 after DRM.

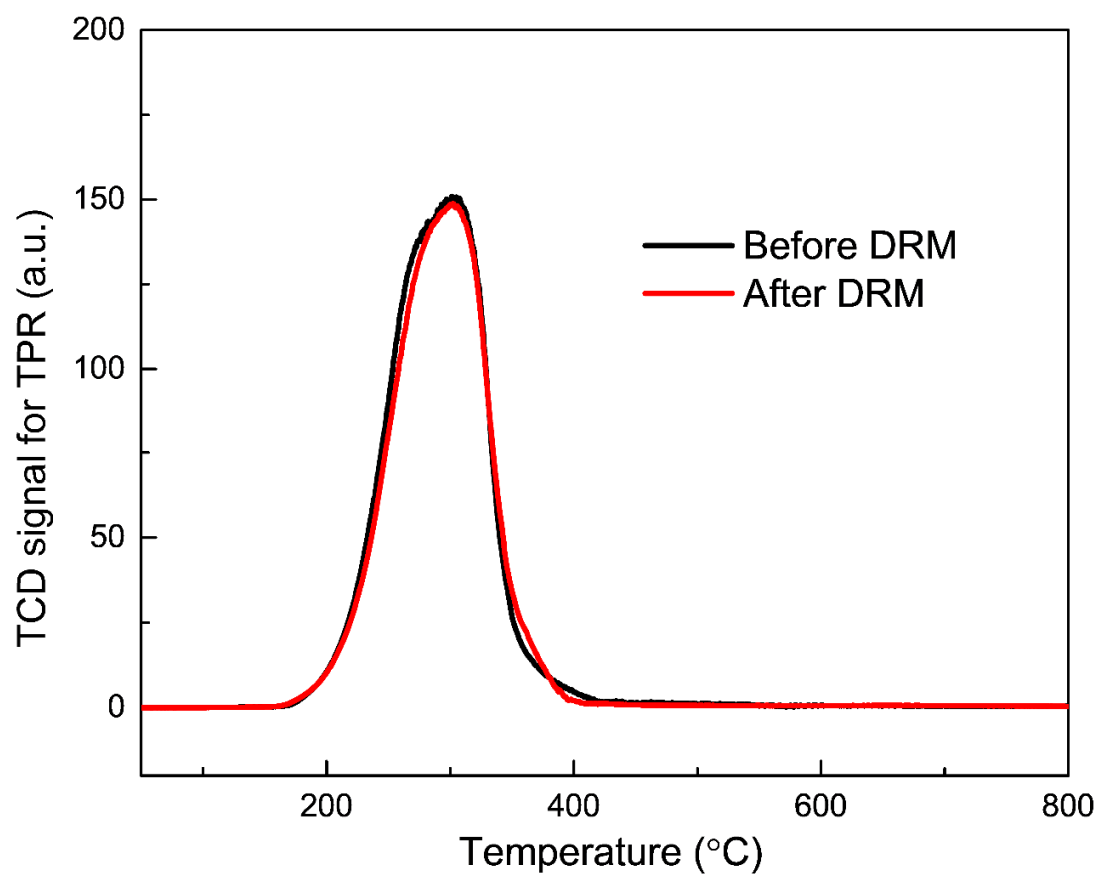


Figure S11. H_2 -TPR of CuO-1000 before DRM and after DRM, the samples were degassed at 350 °C for 2 h with 50 mL/min of He.

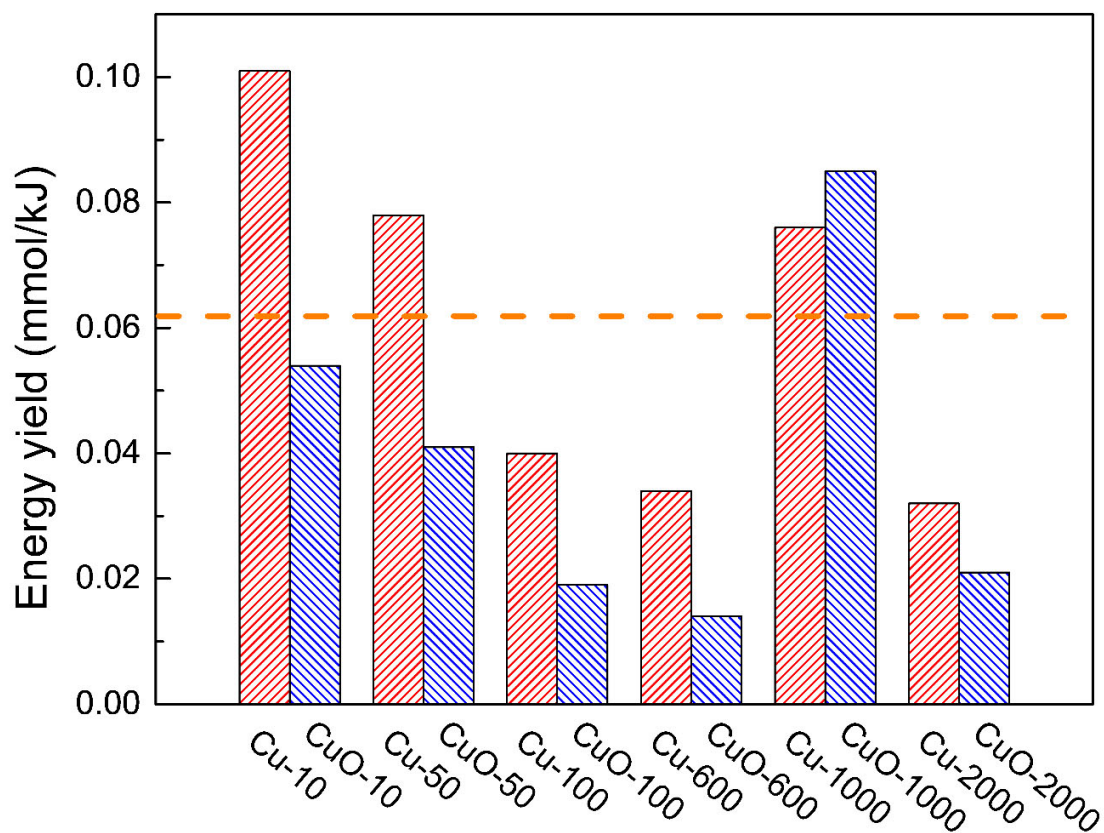


Figure S12. Energy yield in plasma-catalytic dry reforming of 3D porous Cu and CuO samples with different pore sizes. The dashed line is the energy yield of the empty reactor only with plasma at the same gas flow rate.